

Furnace Atomization Plasma Emission/Ionization: Review of an Underutilized Source for Atomic and Molecular Spectrometry

R.E. Sturgeon

Contribution from: National Research Council Canada, Institute for National Measurement Standards, Ottawa, Ontario, Canada K1A 0R9.

Received: September 7, 2004

Accepted (in revised form): November 16, 2004

Résumé

FAPES est une source combinée consistant en un plasma à fréquence radio couplé capacitivement et formé entre un tube de graphite et une électrode électrisée disposée axialement. Elle fonctionne comme une décharge lumineuse oscillant rapidement et générée à pression atmosphérique. FAPES combine les avantages d'un atomiseur à four de graphite avec ceux d'un plasma couplé capacitivement. De l'information multi-élémentaire est disponible dans le mode d'émission, pour les éléments excités dans le plasma, ou dans le mode de spectrométrie de masse, pour les éléments ionisés dans le plasma. La source est aussi ajustable car des informations moléculaire et atomique peuvent être obtenues en modifiant l'énergie du plasma. Une revue est faite des caractéristiques du plasma et des mécanismes d'excitation et d'ionisation ainsi que des coefficients analytiques de mérite dans les modes de détection d'émission et de spectrométrie de masse. La source continue d'être sous-utilisée en spectrométrie atomique analytique à cause du petit nombre d'utilisateurs et du manque d'information sur les applications.

Abstract

FAPES is a combined source consisting of a capacitively coupled radiofrequency plasma formed between a graphite tube and an axially placed

powered electrode. It functions as a rapidly oscillating glow discharge sustained at atmospheric pressure. FAPES combines the advantages of the graphite furnace atomizer with those of the capacitively coupled plasma. Multi-element information is available in either an emission mode, from elements excited in the plasma, or in the mass spectrometry mode, from elements ionized in the plasma. The source is also tunable in that both molecular and atomic information can be obtained by altering the energetics of the plasma. An overview of the plasma characteristics and excitation/ionization mechanisms as well as analytical figures of merit in both emission and mass spectrometry modes of detection is presented. The source continues to be underutilized in analytical atomic spectrometry because of the small user base and lack of applications information.

Keywords: review, FAPES, plasma characteristics, ionization mechanisms, emission, mass spectrometry.

Introduction

Analytical techniques utilizing plasma discharges for optical and mass spectrometry provide several advantageous merits, not the least of which include high detection power, multi-analyte coverage, compatibility with a large variety of sample introduction techniques and ease with which tandem sources can be configured. Intensive research efforts within the analytical chemistry community over the past decade have focused on the development of newly configured plasma sources. The aim is to better enable their performance as detectors for the characterization of not only the elemental

* Author to whom correspondence should be addressed:
ralph.sturgeon@nrc.ca

Dedicated to Jean-Michel Mermet on the occasion of his retirement and appreciation of his numerous contributions to analytical atomic spectrometry.

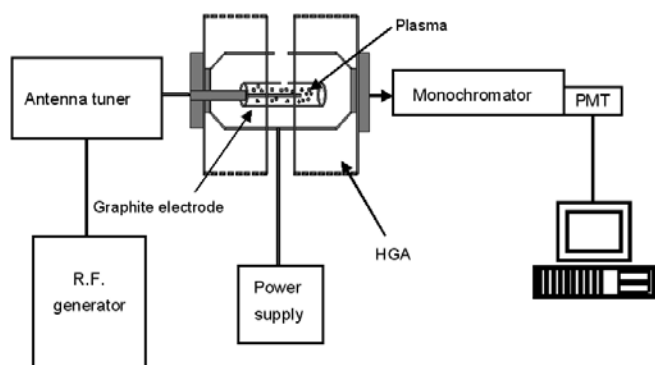


Figure 1. Schematic of the experimental system for FAPES.

composition, but the structure of analyte species (1,2), as well as for their integration into micro Total Analysis Systems, such as the development of chip based microplasmas (3). Microplasmas have recently been reviewed by Karanassios (4).

Of the variety of sources, including microwave induced plasmas, inductively coupled plasmas, DC and rf powered glow discharges, hollow cathode devices and the dielectric barrier discharge, several are based on capacitive coupling of energy into a support gas. Amongst these are the parallel-plate capacitively coupled plasmas (PP-CCP) (5), micro-machined PP-CCPs (6), a capacitively coupled microplasma (CCMP) (7), a microplasma ion source (8), a miniature CC plasma emission detector (9,10) and Furnace Atomization Plasma Emission/Ionization (FAPES) sources (11,12). With the exception of FAPES, there are few data available characterizing these sources with respect to their fundamental properties and analytical capabilities. This review will provide a brief account of the characterization and use of FAPES for trace element analysis in both an emission and mass spectrometric configuration and its application as a detector for the speciation of mercury in environmental samples.

FAPES

The graphite furnace (GF) has enjoyed several decades of prominent use and, although intended primarily for atomic absorption, has also served as a source for atomic emission spectrometry. The low temperatures attained in the GF preclude detection of elements having excitation potentials greater than 4.5 eV and, consequently, combined sources such as the low pressure FANES (Furnace Atomic Nonthermal Excitation

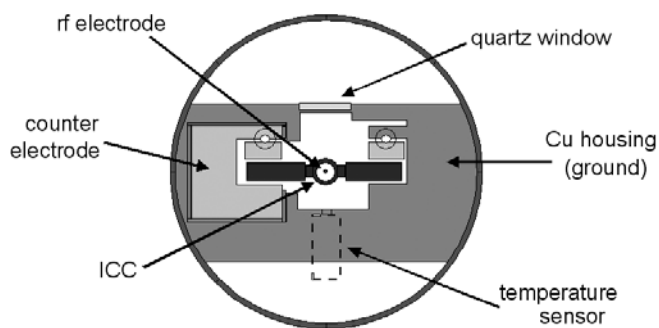


Figure 2. FAPES work head based on a conventional GF.

Spectrometry) (13) and its hollow anode counterpart (14) have been introduced with little success. The low operating pressure leads to reduced analyte residence time and introduces an additional degree of complexity for sampling. Establishment of an atmospheric pressure radio frequency He plasma inside a GF containing a coaxially placed graphite rod antenna provides for a system offering the full advantages of such a combined source (11,12) in that the heated graphite tube serves as an atomizer, and independent non-thermal analyte excitation occurs in the rf plasma, permitting high detection power. The GF can also be operated at atmospheric pressure (permitting conventional sample introduction). A schematic of the FAPES spectrometer is presented in Figure 1, and a detail of the FAPES work head is given in Figure 2. A simple modification of any of the commercially available tube type graphite furnace work heads is required, along with construction of a support for a center electrode which traverses the length of the heated tube and is typically a 1 mm diameter rod of ultrapure pyrolytic graphite coated graphite. A standard N-type rf male connector is attached to the electrode and supplied with rf power from an impedance matching network capable of delivering up to 200 W of power at 13.6, 27 or 40 MHz. The source can then be imaged with a conventional spectrometer or with a CCD camera (15,16). Development of this source has sufficiently evolved that it is commercially available (Model AI 2200; Aurora Instruments Ltd., Vancouver).

The FAPES source is operated in an identical fashion to that of a conventional GF used for AAS. An external sheath gas of Ar is used to prevent oxidation of the heated tube, and an internal flow of He (typically 100 - 200 mL/min) serves as the plasma gas. In practice, 10 - 20 μ L volumes of sample are introduced in liquid form

using a micropipet, whereupon the liquid is evaporated and the residue pyrolysed, as in conventional GF-AAS. The rf power is then applied to the center electrode, a He plasma spontaneously ignited and, following a brief 2-3 s stabilization period, the high temperature atomization stage of the heating cycle is initiated. The sample is volatilized and atomized, and the atomic vapor is excited (and ionized) in the plasma. Atomic and ionic emission lines are monitored and corrected for background. Because of this close operational similarity to GF-AAS, many of the advantageous analytical features of the GF are maintained, including the ability to link the furnace on-line with flow injection (FIAS) chemical pretreatment systems and vapor generation devices for in situ preconcentration schemes. The only requirement is careful attention to the relative placement of the arm of the autosampling unit such that it does not strike the center electrode during insertion (easily avoided by angling the orientation of the dosing hole in the furnace tube).

Plasma characteristics

The temperature and electron number density in high frequency inert gas plasmas are significant figures of merit which are used as indicators to evaluate the performance characteristics of the source, including background intensity, detection limits and susceptibility to interferences (both spectral and non-spectral), and essentially contribute to the robustness of the plasma.

The FAPES source exhibits characteristics similar to that of an atmospheric pressure glow discharge wherein the functional cathode rapidly oscillates between the GF tube wall and the center electrode. The disparity in the mobility between He ions and electrons in the plasma, coupled with the ratio of the effective electrode surface areas and thermionic emission of electrons from the radiationally heated central electrode, results in the induction of a self-bias voltage onto the powered (center) electrode (16,17). Control of this parameter, *via* an imposed DC voltage, provides for a more robust source when detection of the less volatile elements (Fe, Ni, Pt, etc.) is of interest. Both analyte signal intensity and background structure can be improved when the center electrode is shorted to the tube wall (0 V bias potential) to permit a current path for thermionic electrons. Changes in the bias voltage correlate with changes in the intensity of reflected power, as the coupling of the rf energy into the plasma becomes less efficient due to significant impedance changes in the system.

Characteristic temperatures (excitation temperature for support gas and analytes, ionization temperature of analytes, kinetic temperature of plasma gas) measured in the FAPES plasma have been reported in several studies (17-23) from which it is clear that FAPES is a non-LTE plasma. The temperature of the GF during the atomization stage has little effect on these parameters when measures are taken to control the bias voltage induced by thermionic emission. The gas kinetic temperature is typically in the range of 600 - 1000 K, consistent with visual observation of a dull red glow imparted to the center electrode induced by continuous sputtering effected by He⁺ bombardment.

Excitation temperatures for the He support gas are not significantly different from those characterizing MIPs and lie in the range 3000 - 3500 K. As noted earlier, this temperature is influenced by the self bias voltage developed on the center electrode, and when the latter is not controlled, the excitation temperature can vary by up to 700 K over the course of the atomization cycle (otherwise it is limited to 300 K, i.e., a 10 % variation) because potentially large changes in the excitation conditions arise owing to injection of thermionic electrons into the plasma (at tube wall/central electrode temperatures higher than 1800 K). Provided reflected power is deliberately tuned to a minimum (<5 W), the effect of tube wall temperature in the range 300 -1330 K is insignificant. The excitation temperatures for He I are also relatively insensitive to the forward power; a four-fold increase in power (25 to 100 W) produces only a 10 % increase in the excitation temperature (from 2990 to 3300 K). It is the electron density that changes in response to forward power. Increasing the rf generator frequency (13.6, 27, 40 and 54 MHz) for a nominal 50 W forward power plasma was found to increase excitation temperatures by 10 % (from 3260 to 3540 K). The mechanism contributing to this is unclear; several factors could come into play, including changes in the power coupling efficiency into the antenna as the source frequency is changed (although this should not have such a pronounced effect, based on the above data) or change in the skin depth for electron heating as the frequency changes.

Analyte excitation temperatures, as characterized by Boltzmann plots using Fe I and Fe II as the thermometric species, yield temperatures of 2920 ± 180 K and 7610 ± 470 K, respectively. As with other studies of this nature, it must be concluded that there is no unique excitation

temperature for Fe I, it being dependent on the energy levels used for the measurement. The excitation energy derived from high lying levels of Fe I (> 5.5 eV) lies close to that characterizing the Fe II population. Despite 10 % changes in the measured excitation temperature of the He plasma gas over the course of a high temperature atomization transient, excitation temperatures for Fe I do not vary by more than 110 K (i.e., 3 %), suggesting that the mechanisms leading to excitation of the Fe and He are different.

Ionization temperatures for the He plasma gas and several analytes introduced as thermometric species have also been estimated from corresponding Boltzmann plots. For elements having ionization potentials below 8 eV, the degree of ionization is > 50 % and generally increases with increasing rf power. Analyte ionization temperatures of 5900 K were derived from the Saha equation using intensities from Cd and Zn atomic and ionic lines (18). This value compares well with that calculated from the slope of a relationship between the degree of ionization and the ionization potentials for several analytes, i.e., 5280 ± 90 K (23), somewhat lower than the 7500 K characterizing an ICP discharge. The He ionization temperature has been estimated to be in the range 9300 K (24), consistent with a weakly ionized plasma ($\alpha = 5.5 \times 10^{-6}$).

Ar and mixed gas plasmas

Mixed gas plasmas can also be sustained in the FAPES source, most such measurements being undertaken with Ar (19,22,25). Despite the lower ionization potential for Ar, ignition and maintenance of a pure Ar plasma in the FAPES source is more difficult to achieve than when He is used because of the higher *rate* of ionization of He (26). The Ar I excitation temperature is comparable to that of He I, i.e., 3510 ± 150 K at 50 W power (25). Whereas detection of Ar II emission from atmospheric pressure Ar ICPs has not been reported, low pressure glow discharge sources have characteristic Ar II excitation temperatures of 25000 - 50000 K. In this respect, the atmospheric pressure FAPES source appears quite energetic compared to that of an ICP because, although weak, Ar II emission lines can be detected, and an Ar II excitation temperature of 32900 ± 3000 K was obtained in pure Ar. Apparent Ar II temperatures decrease as He is admixed with the plasma gas due to a selective enhancement of the state populations of lower lying levels of Ar II (quartet system), resulting in a greater slope to

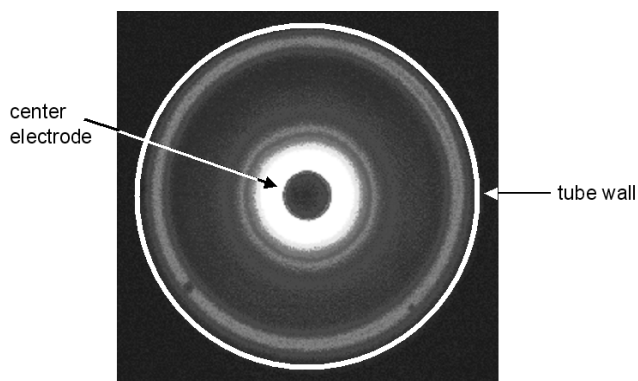


Figure 3. Cross-sectional distribution of the He 667.82 nm line intensity obtained with the graphite tube at room temperature, a forward rf power of 50 W and a 0 V bias imposed on the center electrode. (A) false colored image and (B) three dimensional response surface.

the Boltzmann plot and an apparent decreased temperature. When operated in Ne, an excitation temperature of 4330 ± 80 K is obtained (25). Analyte ionization temperatures in the Ar plasma are on the order of 5200 K (25), not vastly different from that in a pure He plasma.

Electron number densities in the FAPES source have been estimated from measurement of the Stark broadening of the H_{β} line profile at 486.133 nm using high resolution optical emission spectroscopy (18) and also from Langmuir probe data (27). Forward rf powers of 50, 75 and 100 W yielded values of $(6.7 \pm 0.8, 8.1 \pm 1$ and $9.6 \pm 1.2) \times 10^{13} \text{ cm}^{-3}$, respectively, based on Stark measurements and $8.1 \pm 1.2 \times 10^{13} \text{ cm}^{-3}$ at 50 W based on probe data. Both sets of data reflect a weakly ionized plasma that may be subject to strong interferences from the injection of easily ionized species and highlight the important role played by thermionic electrons generated at high GF temperatures and the influence of the bias voltage on analytical performance.

Measurements of these characteristic temperatures and electron densities must be tempered with the knowledge that the FAPES source is highly structured. Figure 3 presents a cross-section of the source imaged with the 667.82 nm He I emission line by a CCD camera. An intense region of plasma surrounds the center electrode along with a diffuse outer ring close to the tube wall, with comparatively little emission in the intermediate region. The intensity of the plasma surrounding the center electrode is approximately 20-fold larger than that of the outer ring, a consequence of their relative surface areas. Although not evident in this

figure, an approximately 90 μm thick dark space exists between the inner tube wall and the diffuse plasma next to it. These features are a consequence of the establishment of negative glows at both surfaces which shift positions and are temporally associated with that electrode serving as the cathode during each half cycle of the applied rf power. Thus, two plasmas exist in the FAPES source, lending it substantial radial inhomogeneity which can be influenced by the dc bias.

Analytical Characteristics

FAPES has been used for analysis of samples for total trace element content and detection of molecules, as well as for speciation, wherein applications have focused on the determination of methylmercury. Transient emission signals generated during the high temperature atomization cycle in the FAPES source are similar to those recorded with graphite furnace atomic absorption (GF-AAS) in terms of their general shape and half-width, although residence times are somewhat shorter because of the more rapid diffusive loss of the analyte atoms in the convective flow of He (28). Estimated appearance temperatures for all elements studied to date (except P) are in good agreement with those published in the GF-AAS literature. For P, the appearance temperature is about 400 K lower than its absorption counterpart, as it is believed that excited P atoms arise from plasma-induced dissociation of volatile molecular phosphorus-containing species; this also accounts for the loss of sensitivity for this element if the plasma is permitted to stabilize prior to sample atomization (2). In the absence of the plasma, no signals can be generated for elements such as Cd, Pb and Bi, indicating that thermal excitation by the hot tube wall plays no role in the excitation process. The effect of forward plasma power (50 - 75 W) is such as to expand the visual volume of the plasma, increase analyte emission intensity and temporally shift the transient to earlier times. The center electrode is primarily responsible for these effects, as it serves as a primary condensation site for analyte desorbing from the (initially) hotter tube walls, after which secondary desorption occurs as the system approaches thermal equilibrium (15).

Plasma background

There are numerous sources of background in this source: continuous radiation from free-free and free-bound transitions, quasi-continua from line wings,

molecular bands from the discharge gas impurities or from reaction products between such impurities and sample constituents, spectral lines emitted by free atoms or ions of the discharge gas or its impurities, spectral lines emitted by free atoms or ions of the concomitants in the sample, and blackbody radiation from the heated tube wall and center electrode. Wavelength scans from 200 - 500 nm point to highly structured background over most of this range (28,19), arising from intense molecular bands of CO, CO⁺, CN, NO, NH, OH, N₂ and N₂⁺ as well as lines from He I and Ar I; the relative intensities of these bands are dependent upon the plasma gas used for excitation (12). The primary source of these is impurities in the plasma introduced by ingress of atmosphere through the sample dosing hole of the furnace. Beyond 500 nm, the plasma background is relatively structureless, apart from some discharge lines. The intensities of these features vary with the temperature of the tube wall (e.g., NO decreases, whereas CO⁺ increases with temperature), reflecting the increasingly reducing atmosphere within the furnace. As with any emission spectrometer, use of high resolution optics coupled with rapid dynamic background correction or, more appropriately, an "electronic photoplate" detector, such as a CCD or CID, can effectively deal with such issues.

Figures of merit

Table 1 compares the absolute limits of detection (LOD) obtained for a number of elements using FAPES with corresponding data for GF-AAS, ICP-OES and FANES. The LODs are based on a 3-sigma criterion estimate of the standard deviation of repetitive measurements of the background or blank signal intensity. In general, detection power lies in the pg range. Room for significant improvement in these data should be expected with use of more efficient transfer optics, dynamic background correction, a high resolution spectrometer, platform atomization, chemical modifiers and an isothermal (e.g., two-step or integrated contact cuvette) furnace. All of the advances made in the use of the stabilized temperature platform furnace concept currently so important to the field of GF-AAS (30) can be conveniently utilized with the FAPES technique. For the less volatile elements, such as Cr, the LOD can be improved 3-fold by utilizing an isothermal furnace to ensure more complete vaporization/atomization (31), whereas for the more volatile elements, application of

Table 1. Peak Height Detection Limits for FAPES Source, pg

Element	Wavelength, λ	FAPES ^a		GF-AAS ^b	ICP-AES	FANES ^c
		He	Ar			
Ag	328.1	0.60	0.70	0.5	3	0.4
As	278.0	5.6	--	20		
B	249.8	903		1000	1.5	1.0
Be	234.8	5.0		1		
Bi	306.7	25		10		30
Al**	309.3	5.5		4		15
Cd*	228.8	0.07		0.3		0.4
CdII	214.4	28	13			
Co	240.7	12	16	2		
CoII	238.9	94	12			
Cr	357.9	17**	50	1		4.0
CrII	283.6	87	27			
Cu	324.8	0.86	1.3	1	2	1.0
Fe	248.3	0.6	0.4	2		4.5
FeII	259.9	73	25		1.5	
Mg	285.2	0.41	0.47	0.5		
MgII	279.6	0.38	1.4		0.1	
Mn	279.5	2.4	3.0	1		
MnII	257.6	12	0.5		0.3	
Ni	232.0	52	14	10	5.5	1.5
P	253.6	94		3000		
	214.9					210
Pb*	283.3	0.15		5		0.3
Pt	265.9	130		50	20	
Se	196.0	460		30	37	800
S (CS)	257.6	1100				
Sn**	284.0	6.1		20		
Zn	213.9	1.1	1.1	0.1	0.9	2.0
ZnII	202.6	100	8.6			

*Ir permanent modifier; **Two-step furnace; ^aData compiled from References 17, 19, 25, 28, 31 and 33; ^bReference 53; ^cReference 13

platform and palladium modification techniques can also improve LODs to the same extent (32), but the relatively massive amounts of modifier introduced may quench the plasma, as there is a tendency for the discharge to arc between the center electrode and their site of deposition. Permanent modifiers, such as iridium, introduced prior to the analysis by thermodeposition, electrodeposition or

sputtering, persist in the atomizer for numerous atomization cycles and effectively accomplish analyte/matrix modification without the need to repetitively add them and without the problem of plasma quenching. In this manner, the LODs for volatile elements such as Cd and Pb were improved by more than an order of magnitude (33).

Linear ranges of calibration curves for the FAPES source are somewhat shorter than expected for an emission source and typically span only three decades (28), not significantly different from those for GF-AAS. It is possible that self-absorption may limit the range in this system because of the large temperature gradient that exists between the center and ends of the furnace, but, more likely, a non-linear response is achieved in relating the mass of analyte to its degree of atomization or desorption efficiency into the gas phase; this presents a fundamental limitation to the technique. This is in accord with the observation that marginal improvements in linear range are achieved when the FAPES workhead utilizes an integrated contact cuvette for atomization (31). The non-homogeneous distribution of analyte species over the cross-section of the graphite tube should not impact the linear range provided that such distributions remain invariant to analyte mass and a reproducible distribution is attained with every heating cycle.

The application of mixed gas plasmas consisting of He and Ar results in increased excitation temperatures arising from collisional exchange of internal energy between excited states of Ar and He (25) and leads to twofold increases in the analyte line intensities, but LODs are substantially unaltered for atomic transitions due to increased background (i.e., noise) associated with the less stable Ar-containing plasma. By contrast, a substantially enhanced ionization temperature (22,25) increases response from ionic transitions by an order of magnitude and is of relevance to the FAPIMS technique (see below). Several factors should be considered when comparing the performance of mixed gas plasmas for FAPES (25): all He plasmas are easily ignited at room temperature upon application of the forward power and remain stable at flow rates as low as 50 mL/min He. Argon plasmas are difficult to ignite and they must first be established in He and converted to an enriched Ar content, following which they are stable only at low forward powers (< 40 W) and high plasma gas flow rates (500 mL/min). The lifetime of the graphite center electrode is severely attenuated in an Ar plasma: from

typically 200 high temperature atomization cycles to only 50-60 such cycles as a consequence of hotter operating temperature and increased sputter damage. Significant enhancements in ionic emission intensity accrue (10 - 40-fold) when Ar is present in the plasma (cf. Table 1), but improvements are less noticeable for atomic lines.

Applications

As with the FANES technique, analytical applications of FAPES to real samples have been limited to date because of the absence of a user base. The performance is influenced by the sample matrix, as this alters the plasma working conditions such that analyte response suffers interference effects (32,33), especially from easily ionized elements (34-37). The presence of easily ionized elements (EIEs) alters the discharge characteristics of the plasma, as evidenced by the fluctuations noted in the self-bias voltage during vaporization of sodium, although the magnitude of the reflected power transient is not altered, even during atomization of up to 160 μg of NaCl (17). Thus, interferences do not arise as a result of decreased power delivered to the plasma. As is common for tandem sources, the extent of interference by EIEs is proportional to the degree of temporal overlap of the gas phase populations of analyte and interferent in the observation volume, which is related to the relative volatilization temperatures and residence times of the species considered. The major causes of EIE interferences in the FAPES source are loss of power radiated by the excited matrix vapor components, alteration of the electron energy distribution function by the injection of low energy electrons from the ionization of the EIE and attenuation of the plasma electron energy through collisional dissociation of molecular matrix vapor (36).

Control of EIE interferences in FAPES can be achieved by clever front end chemistry on the sample to remove or minimize the amount of matrix injected into the source, operation at higher forward powers to help "buffer" the effect of concomitants, use of Ar plasmas instead of He to achieve intrinsically higher plasma electron density (27,38), the application of platform and chemical modification techniques, higher rf frequencies which may dissipate more power into the negative glow region (19,39) and dynamic tuning to minimize reflected power losses (such as by use of a free-running rf generator).

Use of several of these measures, coupled with calibration by the method of additions, permitted the

accurate determination of Cd and Pb in complex digests of sediments and biological tissues (33).

Excitation mechanisms

The introduction of atoms in their ground state into the FAPES plasma occurs during the atomization step; subsequent excitation and ionization of the atom depend on the nature of the plasma gas. The energy distribution of primary electrons, energy levels and densities of metastable atoms as well as the density and kinetic energy of ionized gases play important roles in determining excitation and ionization of analytes. It is thus necessary to identify the key species produced in He and Ar plasmas.

In an Ar FAPES plasma at atmospheric pressure there are metastable atoms ($4s\ ^3P_2^o$, 11.55 eV, and $4s\ ^3P_0^o$, 11.72 eV), metastable molecules (10.2 eV), ground state ions ($3p^5\ ^2P_{3/2}^o$, 15.76 eV), metastable state ions ($3p^5\ ^2P_{1/2}^o$, 15.94 eV), molecular ions (14.0 eV), excited atoms occupying a range of energy levels ($11.83\ \text{eV} < \text{Ar}^* < 15.76\ \text{eV}$), approximately 1×10^{15} electrons cm^{-3} , photons, as well as the molecular impurities noted earlier. In the corresponding He plasma there are metastable atoms ($2s\ ^3S_1$, 19.82 eV and $2s\ ^1S_0$, 20.61 eV), ground state ions ($1s\ ^2S_{1/2}$, 24.59 eV), metastable molecules ($2s\ ^3\Sigma_u^+$, 13.3-15.9 eV), molecular ions ($2s\ ^2\Sigma_u^+$, 18.3-20.5 eV), excited atoms occupying a range of energy levels ($20.61\ \text{eV} < \text{He}^* < 24.59\ \text{eV}$), an electron density of approximately $8 \times 10^{13}\ \text{cm}^{-3}$, photons and molecular impurities similar to those found in the Ar plasma.

Although little is known of the excitation and ionization processes in the FAPES source, mechanisms and models for other plasmas, such as the ICP, MIP and glow discharge source, have been reported. A cursory examination of these models highlights the importance of several general analyte excitation/ionization schemes involving the participation of plasma gas species: collisional excitation by electrons; Penning ionization/excitation with metastable rare gas species (although evidence also suggests that, in the ICP, argon atoms excited to levels above the metastable states also participate in Penning reactions) and charge transfer ionization and excitation collisions (Duffendack reaction) involving asymmetrical charge transfer between plasma gas ions and analyte atoms which leads to the production of excited-state analyte ions. De-excitation processes appear to be dominated by radiative decay and electron

recombination.

The intensity of an emission line from an analyte atom is proportional to the state population of the excited level from which the transition originates. The upper energy levels for most of the excited states of the atomic lines of analytes studied to date are less than 6 eV. Direct population of the excited states of any of the analyte atoms is unlikely to occur *via* efficient exchange of internal energy during collisions with any of the He or Ar plasma gas species. The energy defects for the various collisional excitation scenarios are too large for all of the elements studied. As a consequence, it may be assumed that excitation of all measured analyte atomic lines occurs primarily by (energetic) electron impact with ground state atoms or *via* radiative recombination, in which capture of an electron by an analyte ion results in a highly excited state of the atom which subsequently undergoes radiative cascade or collisional thermalization to populate the level in question. The relative intensities of all atomic lines of the analytes investigated to date are enhanced as the volume fraction of Ar increases in the mixed gas plasma. This is in accord with the increasing electron density likely to occur in moving from pure He to pure Ar. The extent of the emission intensity enhancement should then be related to the excitation energy of the upper level involved in the transition, and this is found to be approximately the case. As noted earlier, there are a variety of molecular species in the plasma, and they may play some role in the excitation of analyte atoms (22).

Two processes generally dominate production of excited state ions in analytical plasmas: Penning and Duffendack reactions. Collisional transfer of the internal energy of any rare gas species to directly populate the measured excited levels of most ions is impossible in the He plasma due to the large energy defects. Excitation of high lying states followed by radiative cascade may account for some fraction of the level population, although this process would be anticipated to be inefficient due to the many branching ratios.

In the case of Cr II, for example, collisional population of any high lying levels by interaction with various He species is spin forbidden by the Wigner rule. Electron impact ionization/excitation thus appears to be one of the few routes available to account for emission from the measured Cr II ($4p\ z\ ^6F^o_{11/2}$, 283.6 nm, 12.69 eV) level in He plasmas. Increases in the intensity of the Cr II line with increased Ar content of the plasma could be linked to the 10-fold greater electron density in this plasma.

Penning ionization/excitation to directly populate the Cr II $4p\ z\ ^6F^o_{11/2}$ level (283.6 nm, 12.69 eV) where the collision partner is an excited state Ar atom (3P_1 , 13.33 eV) is also an attractive possibility, wherein spin conservation is achieved through the release of a free electron in the ionization process. Such a scenario would account for the rise in emission intensities from the atom and ion lines in Ar plasmas as well as the corresponding increase in degree of ionization. Participation of excited state Ar atoms in such processes may occur despite their short lifetime because of their continual overpopulation (with respect to the ground state) *via* interaction with Ar metastables. On the other hand, ionization and excitation of Cd atoms may be accounted for from a consideration of a limited number of potential reactions. The energy levels for Cd II suggest population of the $5p\ ^2P^o_{1/2}$ level in He plasma may occur by radiative/collisional cascade from upper levels which are excited in collisions with excited state He atoms, where a manifold of overlaps appears accessible. These energy transfers cannot be considered viable as they all violate the Wigner spin conservation rule. Collision with He_2^m is also an unlikely scenario, but charge transfer from He^+ may be considered to populate the upper Cd II levels. Approximately half the product Cd^+ ions excited are in the five high-lying $9p\ ^2P$, $8d\ ^2D$, $6g\ ^2G$, $6f\ ^2F$ and $9s\ ^2S$ states, the remaining being distributed between other levels of Cd^+ down to a few eV below the energy of the He^+ ion. Collisional equilibration will serve to populate the measured $5p\ ^2P^o_{1/2}$ level.

As the Ar content of the plasma is increased, emission from the Cd II $5p\ ^2P^o_{1/2}$ level is enhanced, possibly as a result of direct collisional population of the measured $5p\ ^2P^o_{1/2}$ level, as well as *via* a Penning ionization reaction with Ar^* (the Ar $5p\ ^3D_2$ level provides an intense emission line in the FAPES source at 430.0 nm). Direct collisional population of the measured level in the Ar plasma would account for both the substantially enhanced intensity of the 226.5 nm Cd II emission line as well as the significantly increased degree of ionization.

Substantial increases in emission intensity from both the atomic and ionic lines of Mg occur when the plasma gas composition is altered to contain more Ar. Ionization of Mg in the He plasma may arise as a result of Penning reactions with both He^m (into the $6s\ ^2S_{1/2}$ Mg II level) and He^* (into the 9, 8 and 7 s, p and d levels of Mg II) species (spin conserved with the liberated electron), followed by collisional equilibration to the measured $3p$

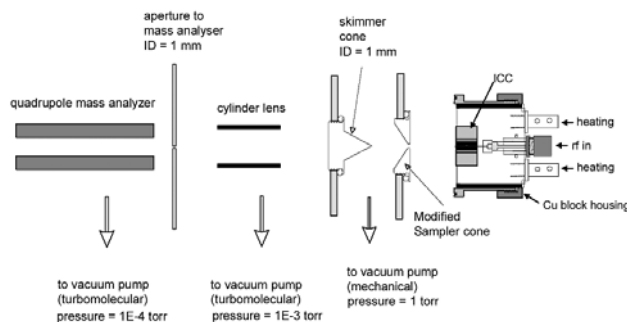


Figure 4. Schematic of FAPIMS instrumentation.

$2P_{3/2}^o$ level (albeit through a large manifold of transitions which makes the overall process inefficient). However, in the presence of Ar, charge transfer reactions have been shown to directly overpopulate the Mg II $4s\ 2S_{1/2}$ and $3d\ 2D_{5/2}$ levels which can collisionally or radiatively equilibrate with the measured $3p\ 2P_{3/2}$ level. Although the endothermic energy defect can be overcome in the Ar ICP by considering the thermal energy (kT) of the heavy particles to be on the order of 0.5 eV (6000 K), such an excess is not available in the FAPES source even with the furnace at its maximum atomization temperature. It is not surprising then that no emission is detected from the Mg II at 292.9, 293.7, 279.8 or 279.1 nm lines, arising from these 3d and 4s levels. Alternatively, the Mg II $3p\ 2P_{3/2}^o$ level may be populated by Penning reaction with excited Ar atoms and *via* electron impact processes [the Ar* transition produces an intense line at 696.5 nm ($4p\ 3P_1$, 13.33 eV) in the FAPES source]. Such reactions may account for the enhanced ionic emission and increase in the calculated degree of ionization with Ar-based plasmas.

The degree of ionization is greater than 70 % in an Ar plasma for elements having an ionization potential below 8 eV, making application of such mixed gas plasmas to enhance the capabilities for use of this source for mass spectrometry attractive (40).

FAPIMS

The capacitively coupled FAPES plasma also serves as an ion source for elemental mass spectrometry (40-44), as it contains sufficiently energetic species to efficiently ionize elements having ionization potentials as high as 10.45 eV (iodine). As an efficient combined source, FAPES does not suffer potential transport losses of analytes in any interface between an atmospheric

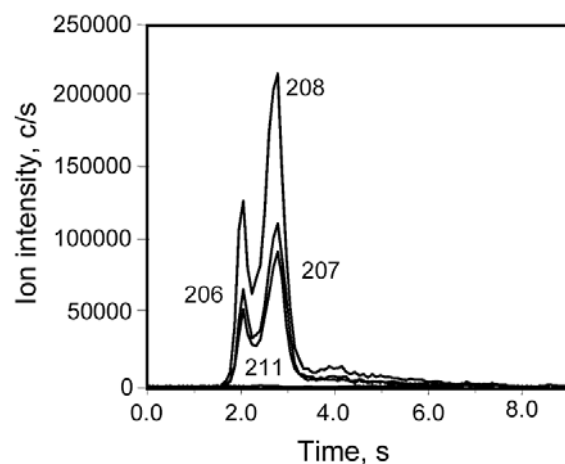


Figure 5. Signal transient for atomization of 1.3 pg of Pb into FAPIMS source. Signal at m/z 211 is presented as an example of the adjacent background.

pressure sampling interface and the ion source based on an integrated contact cuvette (ICC) (14). Figure 4 presents a schematic of such an instrument, christened Furnace Atomization Plasma Ionization Mass Spectrometry (FAPIMS). The only significant change to conventional ICP-MS instrumentation required to support the FAPIMS source is enhancement of the pumping capacity of the interface, as He is used as the plasma gas (40). Sample dosing can be accomplished as with GF-AAS. The background mass spectrum is, as expected, dominated by species such as N^+ , O^+ , OH^+ , H_2O^+/NH_3^+ , H_3O^+ , N_2^+ , NO^+ , O_2^+ , NO_2^+ and N_2O^+ . Their intensities increase with temperature of the ICC. Transient signals can be generated following atomization of discrete introduction of metal ions; the elements tested have spanned a range of ionization potentials from 3.89 (Na) to 13.0 (Cl) eV. The contribution of thermal ionization to the production of signals is negligible. Figure 5 shows response from the atomization of 1.3 pg of Pb introduced into the ICC and atomized at 2000 °C into a 100 W He plasma. Isotopic abundances, calculated from relative signal intensities, are in excellent agreement with natural abundance data (no mass bias correction). The estimated LODs for a number of elements are in the sub-pg to low fg range and are summarized in Table 2, where they are compared with corresponding data for GF-AAS and ETV-ICP-MS. Oxide formation is primarily related to the atomization process in the graphite furnace and detection of PbO^+ for example, can be achieved, consistent with evidence that it is a real species generated within the furnace and does not arise as a consequence

Table 2. Detection Limits for FAPIMS, fg

Isotope	FAPIMS ^a	GF-AAS ^b	ETV-ICP-MS ^c
²⁴ Mg	500	500	NA
⁵⁶ Fe	200	2000	200-10000
⁵⁹ Co	230	2000	20-140
⁶³ Cu	280	1000	420
⁸⁰ Se	300	30000	11000
⁸⁵ Rb	14	5000	NA
¹⁰⁸ Pd	1600	25000	NA
¹¹³ In	20	NA	NA
¹¹⁴ Cd	500	NA	230-500
¹³³ Cs	10	5000	57-100
¹⁷⁴ Yb	2000	NA	NA
¹⁹⁵ Pt	10000	50000	NA
²⁰⁸ Pb	4	5000	2-500
²⁰⁹ Bi	17	10000	NA

NA: not available; ^aReferences 40 and 42; ^bReference 53; ^cReferences 54 and 55

of post oxidation beam extraction reactions (45). Linearity of response of up to 5 decades has been achieved.

FAPIMS, as a source for elemental mass spectrometric analysis, possesses some advantages in that it is highly sensitive, with low-fg LODs and requires only small, discrete samples. Its application to detection of chromatographic effluents is self-evident.

Speciation with FAPES / FAPIMS

It is currently recognized that the determination of the total trace metal burden in most environmental and biological samples provides insufficient information relating to lability, i.e., bioavailability and toxicity, as well as for use in risk assessment scenarios. The separation and quantification of the specific forms of an element defined as to molecular, complex, or nuclear structure, or oxidation state constitutes the field of speciation and atomic spectrometry detectors, when coupled to an appropriate separation technique, currently play a major role in the development of this discipline. In the process,

however, molecular or structural information is lost, and a relative approach to speciation is frequently accomplished by comparison of the temporal responses with those of known standards. This presents a fatal obstacle in the event that an uncharacterized element peak appears in the chromatogram with no retention time match with a known standard. Since no molecular information is available from conventional plasma sources, structural information is lost and identification becomes impossible. Multi-dimensional instrumentation has helped to rectify this problem. A combination of liquid chromatography with electrospray/ion spray sources can be used for measurement of fragment ion patterns, generating (potentially near simultaneous) structural information which can be used to deduce species identity in the absence of a standard. Additionally, "dual mode" analysis, achieved by judicious selection of operating conditions in the atmospheric pressure ionization (API) source interface, permits elemental atomic and molecular information to be obtained on the same sample. In general, this approach is not applicable to trace concentrations of the species of interest, due to a lack of sensitivity.

Additional "soft" ionization sources which provide a dual mode of operation to permit atomic and molecular detection include low power/pressure inductively coupled plasmas, low power microwave induced plasmas (MIPs) and low power glow discharges (46). One of the most illustrative examples of such approaches is the time-gated pulsed glow discharge source coupled with gas chromatography sample introduction and time-of-flight mass spectrometric detection (47). Both atomic and molecular mass spectrometric information can be rapidly (100 Hz) generated in real time by sequentially interrogating the system during the various regimes operative within the GD itself, i.e., recording elemental information during plasma onset, structural information from the molecular spectrum during steady-state operation and detecting molecular ions (M^+ and MH^+) in the after-peak regime.

FAPES also performs well as a detector for quantitation of inorganic and organo-mercury species in combination with gas chromatography for sample introduction (48-51). In such case, the center electrode assembly of the source is modified to permit introduction of GC effluent directly through the center electrode. The latter consists of a 2 mm diameter high purity nickel tube into which the GC column can be inserted. In this manner, the eluted mercury species are directly transported to

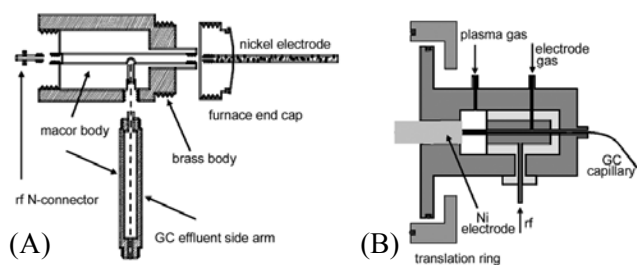


Figure 6. Schematic diagram of the (A) GC-FAPES interface and (B) FAPIMS-GC work head.

the most energetic portion of the FAPES discharge for optimum excitation. Figure 6A illustrates this interface. Biological tissues as well as natural gas condensates have been characterized in this manner and typically require prior derivatization of the mercury compounds to produce the fully alkylated species which are then readily chromatographed. With Grignard butylation of gas condensates, a particularly difficult matrix, LODs for FAPES are comparable to those available with an MIP for methylbutyl- and dibutylmercury, whereas dimethylmercury can be quantitated with the FAPES system but not with the MIP due to plasma instability (49). Precision of replicate measurement for all three species is better than 2 % RSD and, in both sources, the linear range spans three decades. The use of solid phase microextraction (SPME) for sampling of derivatized species simplifies operation further by eliminating the GC solvent load and improving the stability and response by FAPES. Methylmercury and inorganic mercury were determined in several Certified Reference Materials, yielding LODs of 1.5 ng/g and 0.7 ng/g, respectively, following ethylation (50). Use of a propylation reaction in combination with SPME sampling, GC separation and FAPES detection enhanced LODs further (51) to 0.54, 0.34 and 0.23 ng/g for methyl-, ethyl- and inorganic mercury in fish tissue, respectively. These performance features demonstrate that fit for purpose measurements can be achieved with FAPES.

FAPIMS has also been shown useful as a dual mode detector for organometallic speciation, as operation at low power provides for soft ionization, yielding molecular ion information, whereas higher powers generate atomic mass spectra (43). The FAPIMS work head was slightly modified to accommodate sample introduction *via* GC, and is illustrated in Figure 6B. Both forward power to the plasma as well as the spatial or lateral position of the discharge relative to the extraction orifice of the MS could

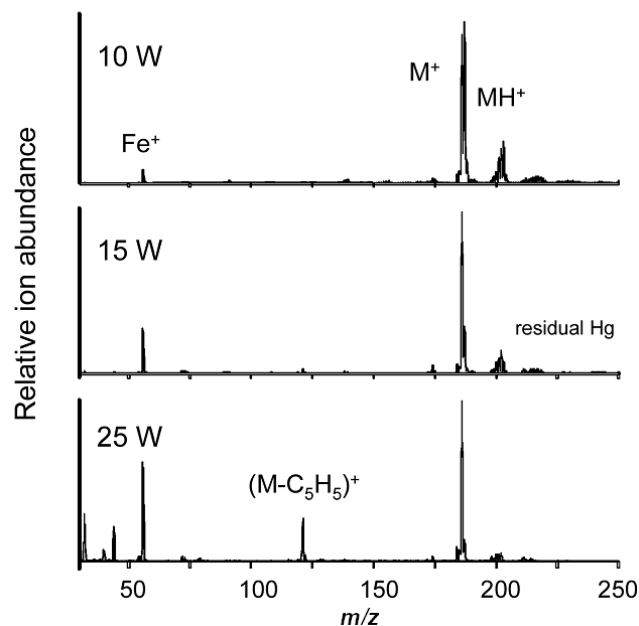


Figure 7. Effect of rf power on relative ion intensities for steady-state introduction of ferrocene vapor into the FAPIMS source.

be varied to effect discriminant detection of either atomic or molecular spectra. This effect is illustrated in Figure 7, which shows the effect of increased rf power (from 10 to 25 W) on the spectra for ferrocene. At 10 W, the spectrum is dominated by the molecular and protonated molecular ions; at high powers (25 W), fragmentation occurs to yield structural information. Suitable electronics could be implemented to achieve this in a rapid, oscillatory manner. In a similar way, changing the lateral position for sampling can be used to move from the most energetic portion of the discharge, located in an annulus around the center electrode, to off-axis regions where the glow is diffuse and molecular ions are plentiful. Dual detection of atomic and molecular species of mercury, lead, arsenic and iron were achieved by altering the rf power, sampler plate voltage, radial position and plasma gas flow rates. A combination of electron impact and chemical ionization appears to be operative for ionization in this source. Detection power in the femtogram range should be easy to achieve.

FAPIMS with GC introduction has also been used for quantitation of organomercury compounds using species specific isotope dilution mass spectrometry (52). A limit of detection of 33 pg was obtained for methylmercury in samples of natural gas condensates following Grignard butylation and GC separation. The strength of this approach is the potential of the FAPIMS

source to provide molecular information useful for identification of new compounds.

Conclusions

FAPES and FAPIMS provide researchers with inexpensive miniplasmas whose performance capabilities are yet unmapped. Applications as an element specific detector for mercury species in both the emission and mass spectrometry mode of operation are clear, but expansion of the scope of elements amenable to this needs to be undertaken. The small user base will likely mean that this capacitively coupled plasma will remain underutilized for the future, despite readily available components from which it can be constructed.

References

1. J.A.C. Broekaert, *Anal. Bioanal. Chem.*, **374**, 182 (2002).
2. J. Franzke, K. Kunze, M. Miclea and K. Niemax, *J. Anal. At. Spectrom.*, **18**, 802 (2003).
3. J.C.T. Eijkel, H. Stoeri and A. Manz, *J. Anal. At. Spectrom.*, **15**, 297 (2000).
4. V. Karanassios, *Spectrochim. Acta, Part B*, **59**, 909 (2004).
5. M.M. Rahman and M.W. Blades, *J. Anal. At. Spectrom.*, **15**, 1313 (2000).
6. A. Bass, C. Chevalier and M.W. Blades, *J. Anal. At. Spectrom.*, **16**, 919 (2001).
7. H. Yoshiki and Y. Horiike, *Jpn. J. Appl. Phys.*, **40**, L360 (2001).
8. C. Brede, S. Pedersen-Bjergaard, E. Lundanes and T. Greibrokk, *J. Anal. At. Spectrom.*, **15**, 55 (2000).
9. R. Guchardi and P.C. Hauser, *J. Anal. At. Spectrom.*, **19**, 945 (2004).
10. R. Guchardi and P.C. Hauser, *Analyst*, **129**, 347 (2004).
11. D.C. Liang and M.W. Blades, *Spectrochim. Acta, Part B*, **44**, 1059 (1989).
12. R.E. Sturgeon, S.N. Willie, V. Luong, S.S. Berman and J.G. Dunn, *J. Anal. At. Spectrom.*, **4**, 669 (1989).
13. H. Falk, E. Hoffmann and Ch. Ludke, *Prog. Anal. At. Spectrom.*, **11**, 417 (1988).
14. N.E. Ballou, D.L. Styris and J.M. Harnly, *J. Anal. At. Spectrom.*, **3**, 1141 (1988).
15. V. Pavski, C.L. Chakrabarti and R.E. Sturgeon, *J. Anal. At. Spectrom.*, **9**, 1399 (1994).
16. V. Pavski, R.E. Sturgeon and C.L. Chakrabarti, *J. Anal. At. Spectrom.*, **12**, 709 (1997).
17. R.E. Sturgeon, V.T. Luong, S.N. Willie and R.K. Marcus, *Spectrochim. Acta, Part B*, **48**, 893 (1993).
18. R.E. Sturgeon, S.N. Willie and V.T. Luong, *Spectrochim. Acta, Part B*, **46**, 1021 (1991).
19. R.E. Sturgeon, S.N. Willie, V.T. Luong and G.J. Dunn, *Appl. Spectrosc.*, **45**, 1413 (1991).
20. C.W. Le Blanc and M.W. Blades, *Spectrochim. Acta, Part B*, **50**, 1395 (1995).
21. M.M. Rahman and M.W. Blades, *Spectrochim. Acta, Part B*, **52**, 1983 (1997).
22. F. Sun and R.E. Sturgeon, *J. Anal. At. Spectrom.*, **14**, 901 (1999).
23. S.Y. Lu, C.W. Le Blanc and M.W. Blades, *J. Anal. At. Spectrom.*, **16**, 256 (2001).
24. R.E. Sturgeon and R. Guevremont, *J. Anal. At. Spectrom.*, **13**, 229 (1998).
25. F. Sun and R.E. Sturgeon, *Spectrochim. Acta, Part B*, **54**, 2121 (1999).
26. T.D. Hettipathirana and M.W. Blades, *Spectrochim. Acta, Part B*, **47**, 493 (1992).
27. R.E. Sturgeon, V.T. Luong and R.K. Marcus, paper No. 272 presented at the 21st annual Conference of the Federation of Analytical Chemistry and Spectroscopy Societies, St. Louis, MO (1994).
28. R.E. Sturgeon, S.N. Willie, V. Luong and S.S. Berman, *Anal. Chem.*, **62**, 2370 (1990).
29. R.E. Sturgeon and S.N. Willie, *J. Anal. At. Spectrom.*, **7**, 339 (1992).
30. W. Slavin, G.R. Carrick, D.C. Maning and E. Pruszkowska, *At. Spectrosc.*, **4**, 69 (1983).
31. K.E.A. Ohlsson, R.E. Sturgeon, S.N. Willie and V.T. Luong, *J. Anal. At. Spectrom.*, **8**, 41 (1993).
32. R.E. Sturgeon, S.N. Willie, V.T. Luong and S.S. Berman, *J. Anal. At. Spectrom.*, **6**, 19 (1991).
33. P. Grinberg, R.C. Campos and R.E. Sturgeon, *J. Anal. At. Spectrom.*, **17**, 693 (2002).
34. R.E. Sturgeon, S.N. Willie, V.T. Luong and S.S. Berman, *J. Anal. At. Spectrom.*, **5**, 635 (1990).
35. D.L. Smith, D.C. Liang and M.W. Blades, *Spectrochim. Acta, Part B*, **45**, 493 (1990).
36. S. Imai and R.E. Sturgeon, *J. Anal. At. Spectrom.*, **9**, 765 (1994).

37. T.D. Hettipathirana and M.W. Blades, *J. Anal. At. Spectrom.*, **8**, 955 (1993).
38. K. Tanabe, H. Haraguchi and K. Fuwa, *Spectrochim. Acta, Part B*, **38**, 49 (1983).
39. R.K. Marcus, *J. Anal. At. Spectrom.*, **8**, 935 (1993).
40. I.I. Stewart and R.E. Sturgeon, *Anal. At. Spectrom.*, **15**, 1223 (2000).
41. R.E. Sturgeon and R. Guevremont, *Anal. Chem.*, **69**, 2129 (1997).
42. I.I. Stewart, R. Guevremont and R.E. Sturgeon, *Anal. Chem.*, **71**, 5146 (1999).
43. R. Guevremont and R.E. Sturgeon, *J. Anal. At. Spectrom.*, **15**, 37 (2000).
44. S.Y. Lu, C.W. LeBlanc and M.W. Blades, *J. Anal. At. Spectrom.*, **16**, 256 (2001).
45. R.E. Sturgeon, D.F. Mitchell and S.S. Berman, *Anal. Chem.* **55**, 1059 (1983).
46. R.K. Marcus, E.Hywel Evans and J.A. Caruso, *J. Anal. At. Spectrom.*, **15**, 27 (2000).
47. C.L. Lewis, M.A. Moser, D.E. Dale, Jr., W. Hang, C. Hassell, F.L. King and V. Majidi, *Anal. Chem.*, **75**, 1983 (2003).
48. M.S. Jimenez and R.E. Sturgeon, *J. Anal. At. Spectrom.*, **12**, 597 (1997).
49. W. Frech, J.P. Snell and R.E. Sturgeon, *J. Anal. At. Spectrom.*, **13**, 1347 (1998).
50. P. Grinberg, R.C Campos, Z. Mester and R.E. Sturgeon, *Spectrochim. Acta, Part B*, **58**, 427 (2003).
51. P. Grinberg, R.C. Campos, Z. Mester and R.E. Sturgeon, *J. Anal. At. Spectrom.*, **18**, 902 (2003).
52. J.P. Snell, I.I. Stewart, R.E. Sturgeon and W. Frech, *J. Anal. At. Spectrom.*, **15**, 1540 (2000).
53. W. Slavin, "Graphite Furnace AAS A Source Book," The Perkin Elmer Corporation, Ridgefield, USA (1984).
54. J.M. Carey and J.A. Caruso, *Crit. Rev. Anal. Chem.*, **23**, 397 (1992).
55. D.C. Gregoire, *Can. J. Spectrosc.*, **42**, 1 (1997).